PHYSICAL REVIEW B VOLUME 10, NUMBER 10 15 NOVEMBER 1974

Ab initio calculation of the pressure-induced $A4 \longrightarrow A5 \longrightarrow A2$(distorted) $\longrightarrow A3$ phase transitions in tin

J. Hafner*

Institut für Theoretische Physik, Technische Hochschule Wien, Wien, Austria

(Received 15 May 1974)

The pressure-induced phase transitions in tin from the diamond ($A4$) to the white-tin ($A5$) and further to a simple face-centered-tetragonal structure continuously deforming upon higher compression towards a body-centered-cubic ($A2$) structure are calculated by means of a first-principles pseudopotential method without adjustable parameters. The critical compressions for the phase changes as well as the structural details of the tetragonal high-pressure modifications are predicted with good accuracy. For very high compression a transition to the hexagonal-close-packed ($A3$) structure is predicted.

I. INTRODUCTION

Pseudopotential and model-potential methods have been applied with considerable success to the problem of the relative energies of different crystal structures of nontransition metals.[1-3] The method has also been extended to calculate the temperature-induced martensitic phase transitions in Li and Na.[4] The application to pressure-induced phase changes has been less successful. Only an *ad hoc* adjustment of the model potential allowed Inglesfield[5] to account for the transition from the orthorhombic ($A11$) Ga I phase to the tetragonal ($A6$) Ga II phase (here and later we shall use the structure notation proposed in the Strukturbericht[6]). The p, T phase diagram of Sr has been calculated by Animalu[7] and by Moriarty.[8] Moriarty's calculation, based on Harrison's[9] first-principles pseudopotential formalism including d-band hybridization, fails to obtain the pressure-induced $A1$-$A2$ transformation. Animalu achieved qualitative agreement with experiment, but unfortunately his somewhat approximate calculation (including uncertain modifications in the model potential) has been disproved by more fundamental calculations using the same type of potentials, yielding $A3$ as the stable structure of Ca and Sr at zero temperature and pressure.[10] Weaire and Inglesfield[11] have speculated about possible reasons for the tetragonal distortion of the Sn II ($A6$) structure, without attempting numerical calculations. Thus the pressure-induced phase changes constitute an open challenge to pseudopotential theory.

The form of Sn which is stable at zero temperature and pressure is the semimetal form, grey tin (α-Sn), and has the cubic diamond structure ($A4$). Under pressure it transforms to the metallic white-tin (β-Sn, $A5$) structure, which is related to the diamond structure by a large compression along a cubic axis. The α-β phase boundary at low temperatures has been investigated by Nikolaev and co-workers.[12] At still greater pressures, there is a transition to a face-centered-tetragonal ($A6$) structure, the axial ratio being about 0.65[13,14] [The face-centered-tetragonal structure is equivalent to a body-centered-tetragonal structure with axial ratio $(c/a)_{\text{bct}} = (c/a)_{\text{fct}} \times \sqrt{2}$]. According to Musgrave,[15] the atoms will be located at the lattice points of a fct ($A6$) lattice if one selects appropriate vibrational modes of the $A5$ structure and considers the positions of the atoms at the moment of maximum displacement. The axial ratio of this hypothetical structure is $c/a = 0.54$. The structural transitions parallel a change from an "ideal semimetal" to a purely metallic behavior. The available experimental information on the p, T phase diagram of Sn is compiled in Fig. 1, the α-β and β-II phase boundaries being extrapolated to the absolute zero of temperature.

II. $X\alpha$-PSEUDOPOTENTIAL THEORY

The present calculation is based upon Harrison's first-principles pseudopotential formalism.[9] In this method, the pseudopotential W is obtained by an exact transformation of the electron-ion potential V. The pseudopotential is optimized in the sense that the pseudowave function is smooth and that a perturbation series in W has optimal convergence. The difficult point is the construction of the convenient electron-ion potential V. Although sometimes treated as if any reasonable approximation were good enough, the nature of this potential (and especially of the core–conduction-band exchange contribution to it) in the outer regions, where it overlaps its neighbors, can have a significant effect on the over-all electronic structure of the crystal. In a recently presented series of papers,[3,19,20] we have studied the use of the $X\alpha$ exchange and correlation approximation[21] for the core-core and the conduction-band–core interactions within the framework of a pseudopotential theory. It was shown that using the optimized exchange parameter α_{vt} of the free atom[22] for the core-core exchange and a smaller parameter $\alpha_{ie} < \frac{2}{3}$ for the conduction-band–core exchange [accounting for the interelectronic nature of this interaction and the overestimate of the range of the exchange interaction in the $X\alpha$ method (cf. Refs. 23 and 20)], good agreement is obtained for the structural and cohesive properties of the simple metals from Li to In. For Sn these calculations imply a value of $\alpha_{ie} = 0.50$ which will be used here.

Exchange and correlation among the conduction electrons are taken into account by using a generalized dielectric function in the random-phase approximation (RPA)

$$\epsilon(q) = 1 + [1 - G(q)][\epsilon^{\mathrm{RPA}}(q) - 1]\,. \qquad (1)$$

There has been much discussion about the convenient form of the exchange and correlation correction $G(q)$. From our foregoing calculations[3] we know that the exact form of this correction is only moderately important for structural and cohesive properties. From our phonon calculations[20] it appears that a Hubbard-Sham-type correction function, adjusted to fit the compressibility sum rule,[24] is most convenient in simple metals, though other forms, e.g., that proposed by Singwi and co-workers,[25] are supposed to have a better theoretical background. We shall not contribute to lasting discussion. The correct $G(q)$ will probably lie between the Hubbard-Sham (HS) and the Singwi-Sjölander-Tosi-Land (SSTL) correction function. In order to be able to investigate possible influences coming from the conduction-electron exchange and correlation, we use both $G(q)$ functions in our work. The total energy of the system may than be calculated using the conventional second-order perturbation theory.[3,9]

This approach might be criticized in two points: (i) In metals with valence $Z \geq 4$, higher-order perturbation terms are generally expected to yield non-negligible contributions to the bonding energy. However, in the present status of the theory, there is no possibility of going beyond the second order in a calculation which retains all the nonlocality and the exchange and correlation contributions to the pseudopotential. In multivalent elements these aspects are certainly equally, if not more, important than higher-order corrections. It is also worthwhile to compare the perturbation parameter $w(q)/E_F$ of Sn [where the orthogonalized-plane-wave (OPW) form factor $w(q)$ is defined by $w(q) = \langle \vec{k} | w | \vec{k} + \vec{q} \rangle$, $|\vec{k}| = |\vec{k} + \vec{q}| = k_F$ for $q \leq 2k_F$; $(-\vec{k}) \parallel (\vec{k} + \vec{q})$ (backscattering) for $q > 2k_F$, and E_F is the Fermi energy]: $w(q)/E_F \leq 0.13$ for β-Sn (atomic volume $\Omega_0 = 181.5$ a.u.[3]), and ≤ 0.22 for α-Sn ($\Omega_0 = 230.6$ a.u.[3]) for all wave-number lattice vectors with nonzero structure factor $S(q)$ with the corresponding values for other metals: $w(q)/E_F \leq 0.03$ for Al ($A1$), ≤ 0.07 for Mg, ≤ 0.17 for Na, and ≤ 0.27 for Li (all three $A3$). It appears that the neglect of higher-order terms is not a very serious restriction for β-Sn, though more important in the α phase. It should also be stressed that for strongly distorted structures such as $A11$ (Ga I), the perturbation parameter increases to 0.35–0.4 in Sn. Such structures are therefore definitely outside the scope of a perturbation approach. (ii) We use a linear, and not a covalent screening function in α-Sn. In the high-pressure modifications, this approach is certainly well justified and it represents the only possibility to construct a single structure-independent pseudopotential. We shall come back to this point when we discuss the stability of the α phase in our theoretical system.

III. STRUCTURAL STABILITY

We have calculated the binding energy of tin at the observed atomic volume of white tin (Ω_0

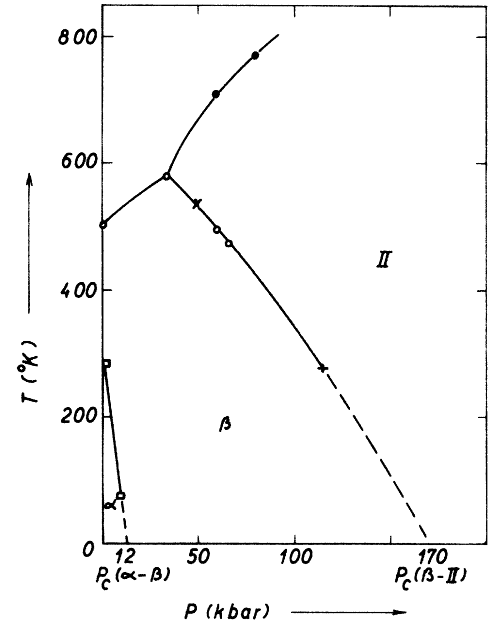

FIG. 1. p, T phase diagram of tin. α–β phase boundary: Nikolaev *et al*. (Ref. 12); β–II phase boundary: ○, Barnett *et al*. (Ref. 13), X, Kennedy and Newton (Ref. 16), +, Stager *et al*. (Ref. 14); melting point: Gschneider (Ref. 17); II-liquidus: ●, Dudley and Hall (Ref. 18).

$= 181.50$ a.u.[3]) and for six additional values of the atomic radius r in the range between 0.85 and 1.15 times the observed radius r_0 in a tetragonally distorted $A4'$structure [the axial ratio c/a was varied over the range 0.25 to 4.0, i.e., including both the $A4$ ($c/a = 1$) and the $A5$ ($c/a = 0.384$) structures], in the simple face-centered-tetragonal ($A6$) structure [$0.3 \leq c/a \leq 3.2$, i.e., including the face-centered-cubic ($A1$, $c/a = 1$) and the body-centered-cubic ($A2$, $c/a = 1/\sqrt{2}$) structures], and in the hexagonal-close-packed ($A3$) structure. It was necessary to consider such large ranges of the axial ratio to guarantee that the absolute minimum of the axial ratio was included. However, it should not be forgotten that for very strongly distorted structures ($A4'$: $c/a \geq 3.0$ or ≤ 0.3; $A6$: $c/a \geq 2.2$ or ≤ 0.4) the perturbation parameter increases beyond 0.3 for lower electron densities (expanded metal), and the second-order approach becomes inapplicable. This restriction is more severe in the $A6$ structure than in the $A4'$ lattice because in the latter case, the structure factor $S(\vec{q})$ vanishes for the shortest vector in the wave-number lattice.

In Fig. 2(a) and 2(b) we represent the OPW form factor $w(q)$ defined above and the energy–wave-

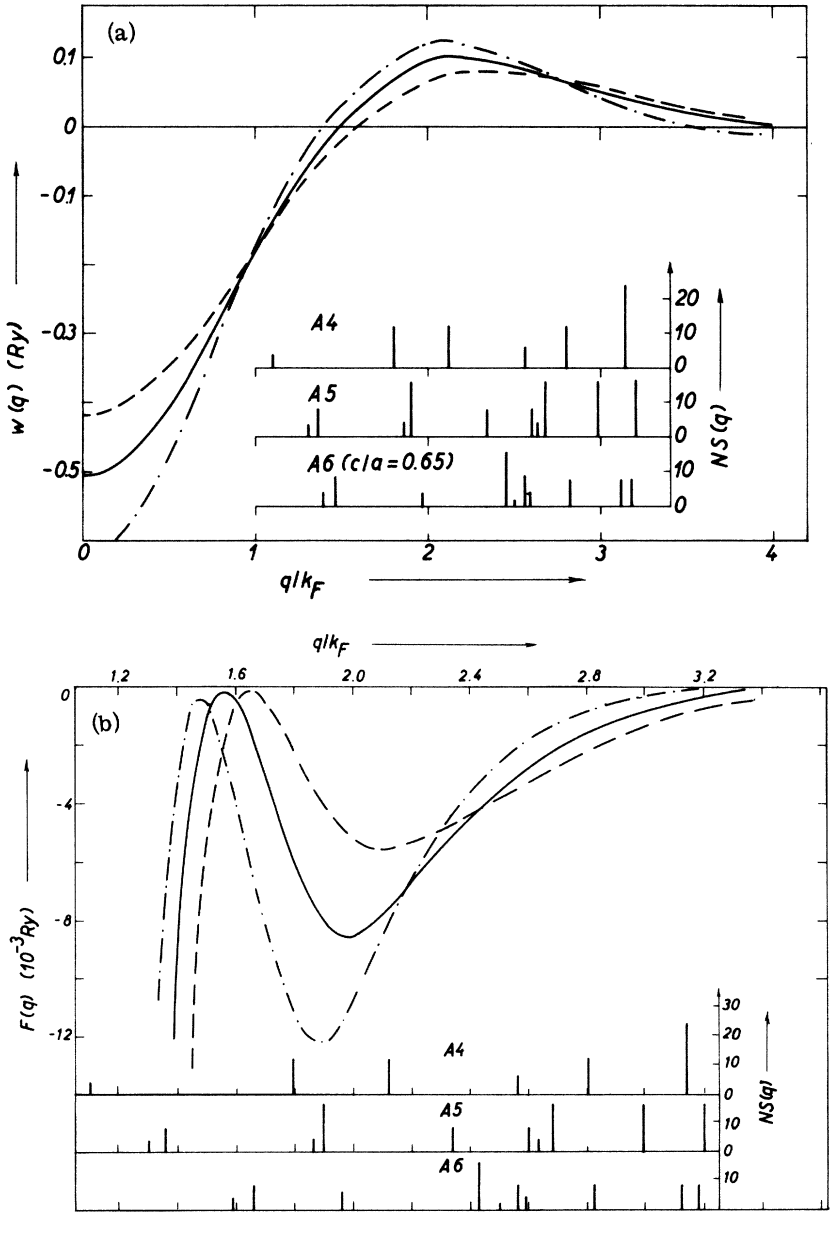

FIG. 2. OPW form factor $w(q)$ and energy–wave-number characteristic $F(q)$ of tin for three different atomic radii: dot-dashed curve, $r = 0.9r_0$; solid curves, r_0 (observed atomic radius of white tin); dashed curve, $r = 1.1r_0$. The distribution of the structural weight $NS(q)$ in the three allotropic modifications is shown in the insets.

number characteristic $F(q)$ calculated with the Hubbard-Sham screening function for three different values of the atomic radius, $r = 0.9$, 1, and 1.1 times r_0. The distribution of the structural weight $NS(q)$ [defined as the structure factor $S(\vec{q})$ times the number of wave-number lattice points with $|\vec{q}| = q$] in the three different phases of tin is indicated. From these figures we can draw a first qualitative indication: when the metal is compressed, the maximum in the characteristic is shifted towards smaller values of q/k_F. Therefore, the contributions to the binding energy of the first shell of reciprocal lattice vectors in the $A4$ lattice and of the first and second shells in the $A5$ structure will be strongly reduced. The close-packed structures become less unfavorable from the point of view of the band-structure energy E_{bs} and much more favorable from the aspect of the electrostatic energy. In multivalent metals, however, the cancellation between electrostatic and band-structure terms is so close that a full calculation of the structural energies is necessary.

In Figs. 3(a)–3(f) we have plotted the structural energy difference relative to the $A4$ structure in the distorted $A4'$ lattice as a function of the axial ratio for atomic radii $r = 0.85r_0$, $0.9r_0$, $0.95r_0$, r_0, $1.05r_0$, and $1.1r_0$. The values of c/a which define the $A4$ and $A5$ structures are indicated, and the horizontal line represents the energy of the $A6$ phase with axial ratio minimizing the energy. The solid lines refer to the results calculated with the Hubbard-Sham (HS) dielectric function, and the broken lines to those obtained with the (SSTL) screening of Singwi *et al.* The binding energy is always stationary with respect to tetragonal distortion in the diamond lattice. In the strongly compressed metal, E has a local maximum for $A4$. When the crystal is expanded, this maximum flattens, and in the case of the SSTL screening it changes even in an absolute minimum. In this case the indirect ion-electron-ion two-body interaction is strong enough to stabilize the diamond structure. In the HS approach, the indirect part of the interionic pair potential is more effectively screened, and a very slight tendency to a tetragonal distortion persists even at the equilibrium volume of grey tin. For a complete explanation of the $A4$ structure higher-order terms have to be considered. Such an approach would be more consistent than the use of a coval-

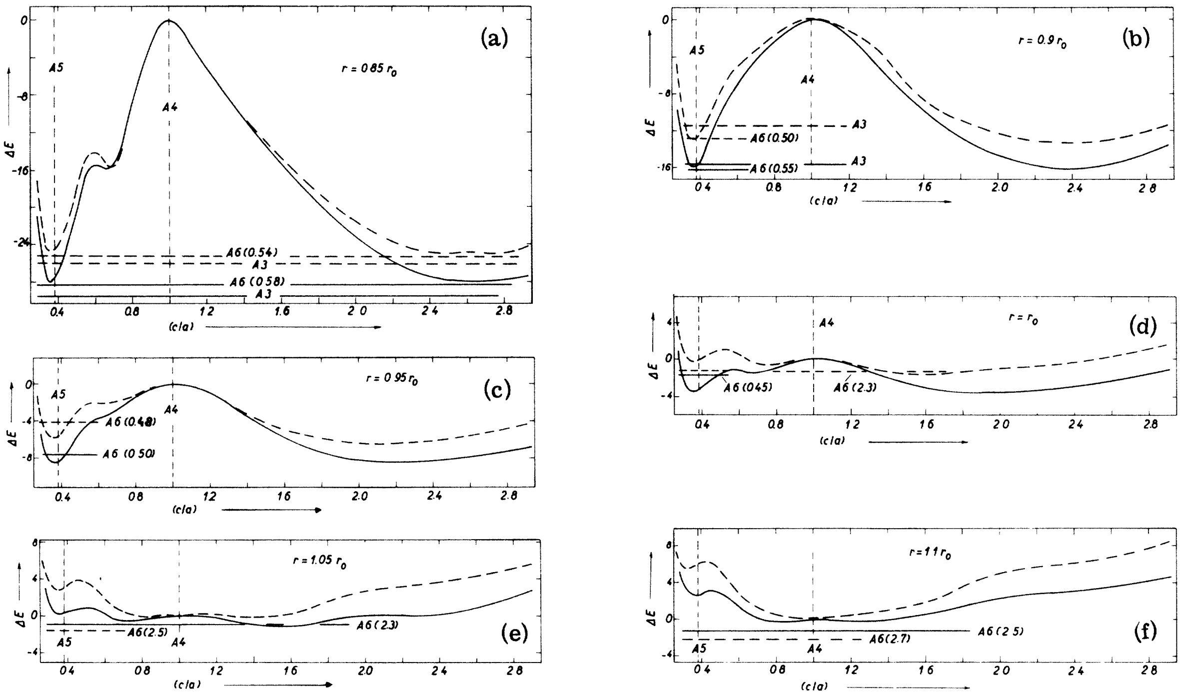

FIG. 3. Structural energy difference relative to the diamond ($A4$) structure ΔE (in 10^{-2} Ry) in a tetragonally distorted $A4'$ lattice for different atomic radii ($r = 0.85r_0$–$1.1r_0$ (r_0 is the observed atomic radius of white tin). Values of the axial ratio c/a corresponding to the $A4$ and $A5$ structures are indicated. The horizontal lines represent the relative energies of the $A6$ (with axial ratio minimizing the energy as given in the parentheses) and $A3$ structures. The solid lines refer to the results calculated with the Hubbard-Shem dielectric function, the broken lines to those calculated with the one of Singwi *et al.*

ent screening function. For the present purpose—the calculation of the pressure-induced phase transitions—it is acceptable to neglect the small tendency to a tetragonal distortion, and the second-order calculation is sufficient.

Independently of the compression, a local minimum in the $E(c/a)$ curves appears at $c/a \simeq 0.365$; this is a bit below the observed axial ratio $c/a = 0.384$ of the β-Sn phase. A second minimum exists for $c/a > 1$, its position and relative depth depending strongly upon the atomic volume. At $r = 1.1r_0$, and $1.05r_0$ the absolute minimum in the energy occurs in the $A4$ structure (if we neglect the small distortions); at $r = r_0$ and $0.95r_0$ the $A5$ structure is the stable one. For $r = 0.9r_0$ and $0.85r_0$ the second minimum at $c/a \sim 2.4$–2.5 becomes of comparable and even greater depth, but in this compression range a face-centered-tetragonal and a hexagonal-close-packed structure, respectively, are still lower in energy. Thus it is evident that the theory is able to explain the observed phase transitions.

Before discussing this point, we shall investigate the stability of the different phases in further detail. For this purpose we consider the electrostatic and band-structure contributions to the binding energy separately. In Fig. 4(a) we represent the Ewald coefficient of a tetragonally distorted $A4$ lattice as a function of the axial ratio. The diamond structure is seen to be very unfavorable from the point of view of purely electrostatic interactions; our calculated $\alpha_{\mathrm{Ew}}(A4) = -1.670856$ confirms Harrison's[9] calculation. The Ewald coefficient is minimized for the white-tin structure, being $\alpha_{\mathrm{Ew}}(A5) = -1.773118$; a local minimum which is only slightly smaller appears in the neighborhood of the reciprocal value of the axial ratio $[c/a(A5) = 0.384]$, $\alpha_{\mathrm{Ew}}(c/a = 2.6) = -1.772917$. It can be easily seen that these values of the axial ratio are very close to those for which the nearest and the next-nearest-neighbor shells in real space coincide ($c/a = 0.365$ and, respectively 2.45). The minima in the Ewald coefficient therefore arise from a higher effective coordination number. That α_{Ew} is stationary in the $A5$ lattice is by no means a contradiction to the result of Brovman and Kagan,[26] who calculated imaginary Coulomb frequencies for some branches. In fact the $A5$ structure is related to the $A6$ lattice through a deformation corresponding to a particular superposition of vibrational modes, and the latter structure has a lower electrostatic energy. Therefore the Coulomb frequencies of these modes have to be imaginary. The band-structure energy [Fig. 4(b)] on the other side has a minimum in the diamond lattice and maxima for $c/a = 0.384$ and $c/a \simeq 2.65$, independent of the atomic volume. The position of the minimum in the total energy therefore depends upon the balance between electrostatic and band-structure contributions. For $r \geq 1.1r_0$, the minimum in the band-structure energy overcompensates the maximum in the electrostatic energy, and $A4$ is the stable structure of tin. When the crystal is compressed, the band-structure energy decreases slowly, the dependence upon the axial ratio remaining the same. The electrostatic energy $E_{\mathrm{es}} = Z^{*2}\alpha_{\mathrm{Ew}}/r_0$ on the other side increases even faster than $1/r_0$ because of the growing effective valence Z^*. For $r \leq r_0$ it is the electrostatic part that dominates the structural energy. For $r = 1.05r_0$ the cancellation is particularly close and neither the $A4$ nor the $A5$ structure appear to be stable. However, as we shall see later, this atomic radius lies in the transition region between the α and the β phase.

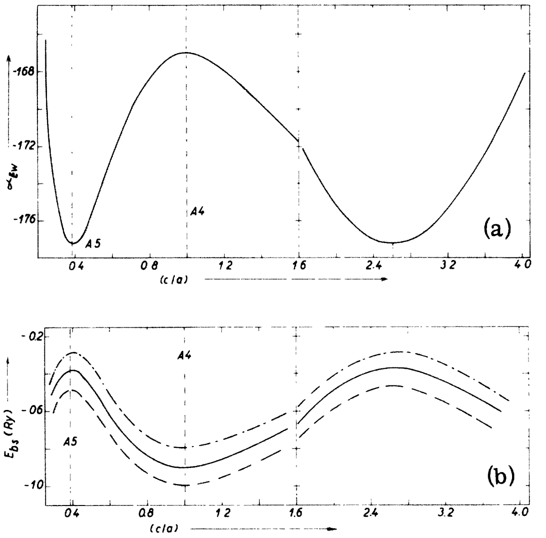

FIG. 4. Variation of the electrostatic and band-structure contributions to the binding energy in a tetragonally distorted $A4'$ lattice as a function of the axial ratio. (a) Ewald coefficient. (b) Band-structure energy E_{bs} for different atomic radii: dot-dashed curve, $r = 0.9r_0$; solid curve, r_0 (observed atomic radius of white tin); dashed curve, $r = 1.1r_0$.

The same investigation has been performed for the $A6$-type lattice. The variation of the Ewald coefficient α_{Ew} with the axial ratio is well known in principle; our results are presented in Fig. 5(a). Two minima appear for the $A1$ and $A2$ structures, the latter being slightly deeper [$\alpha_{\mathrm{Ew}}(A1) = -1.791747$, $\alpha_{\mathrm{Ew}}(A2) = -1.791855$; our results exactly confirm Sholl's[27] calculation]. For $c/a > 1$ and $c/a \leq 1/\sqrt{2}$, α_{Ew} increases steeply. The band-structure energy shows a quite different dependence upon the axial ratio [Fig. 5(b)]: E_{bs} has its maximum value for a close-packed structure, the exact position depending upon the atomic volume. For $r = 1.1 r_0$ and r_0, the $A1$ structure has the maximum band-structure energy; for $r = 0.9 r_0$ a second maximum appears for the $A2$ structure, and for a still greater compression this is the absolute maximum. Here again, the structural energy depends mainly upon the balance between electrostatic and band-structure contributions [Figs. 6(a) to 6(f)]. For $r \geq 0.95 r_0$ the band-structure term dominates. At $r = 1.0 r_0$ and $1.1 r_0$ a very strongly distorted $A6$ lattice ($c/a \simeq 2.4$) even comes out to be energetically more favorable than the $A4$ structure. However, it has been emphasized above that for such severely distorted structures ($c/a \geq 2.2$), the perturbation approach breaks down, and the band-structure energy is overestimated. No physical arguments may be built upon this particular result. On the other hand, the minimum appearing at $c/a = 0.4$ to 0.6 is realistic. With increasing compression it grows deeper and its position is shifted towards greater values of the axial ratio. At $r = 0.9 r_0$ an $A6$ structure with $c/a = 0.55$ (in the HS approach) and 0.50 (in the SSTL approximation) is the stable structure. It is interesting to point out the near coincidence between our calculated axial ratios and that of the hypothetical structure considered by Musgrave.[15] Although our work is not concerned with the transformation mechanism, this result certainly corroborates the ideas of Musgrave. For a still greater compression, the axial ratio increases continuously towards $c/a = 1/\sqrt{2}$, i.e., the structure changes without discontinuity in the atomic volume into an $A2$-type structure.

At the same time, however, the close-packed structures $A1$ and $A3$ become increasingly favorable in the binding energy [cf. Figs. 6(e) and 6(f) and Table I]. At $r = 0.85 r_0$ the $A3$ lattice has the lowest energy. Therefore, a third pressure-induced phase transition from a slightly distorted body-centered-cubic ($A2$) to a hexagonal-close-packed structure ($A3$) occurs in tin. Contrary to the $A4 \rightarrow A5$ and $A5 \rightarrow A6$ (distorted $A2$) transformations, this phase change is not an electrostatic, but a band-structure effect, since both close-packed structures ($A1, A3$) have a higher Ewald coefficient than the $A2$ lattice ($\alpha_{\mathrm{Ew}}(A3) = -1.79163$). The possible occurrence of such a phase transition has in fact been predicted by Evdokimova[28] on the basis of similarity considerations of the p, T-phase diagrams of the group-IV elements C, Si, Ge, Sn, and Pb. Our calculation represents the first theoretical confirmation of these considerations.

The general principle underlying the sequence of transformations $A4 \rightarrow A5 \rightarrow A2$ (distorted $\rightarrow A3$ is the increase in coordination number and packing density (cf. Table II). Within the framework of our pseudopotential theory, this principle is realized not by the increase of the electrostatic contributions alone, but by the balance between ionic and electronic terms. Section IV is devoted to the calculation of the critical data for these transitions.

IV. PHASE TRANSITIONS AND CRITICAL DATA

It is most simple to consider pressure-induced phase changes in terms of the Gibbs free enthalpy $H = E + p\Omega - TS$ as a function of the pressure p.

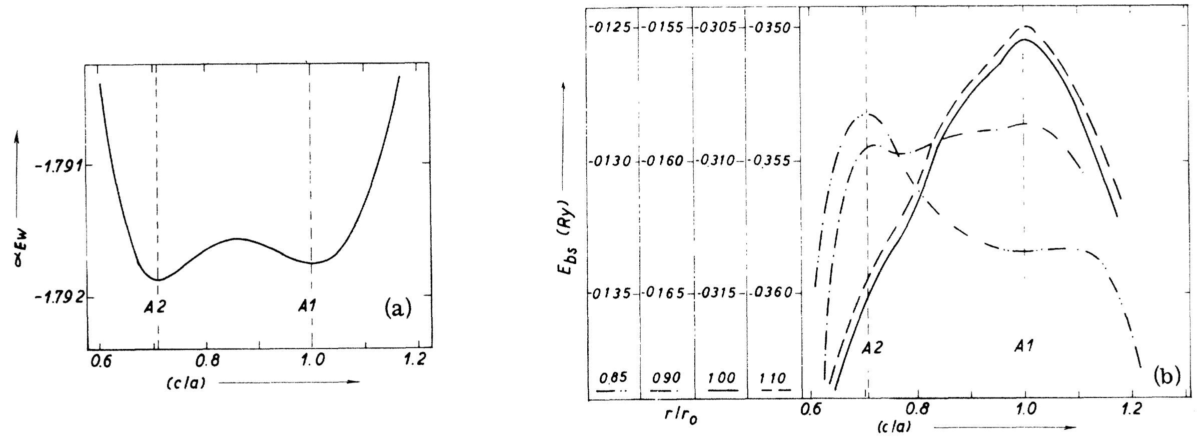

FIG. 5. Variation of the electrostatic and band-structure contributions to the binding energy in an A 6-type structure as a function of the axial ratio c/a. Values of c/a corresponding to the $A1$ and $A2$ lattices are indicated. (a) Ewald coefficient. (b) Band-structure energy E_{bs} for different atomic radii r(r_0 is the observed atomic radius of white tin).

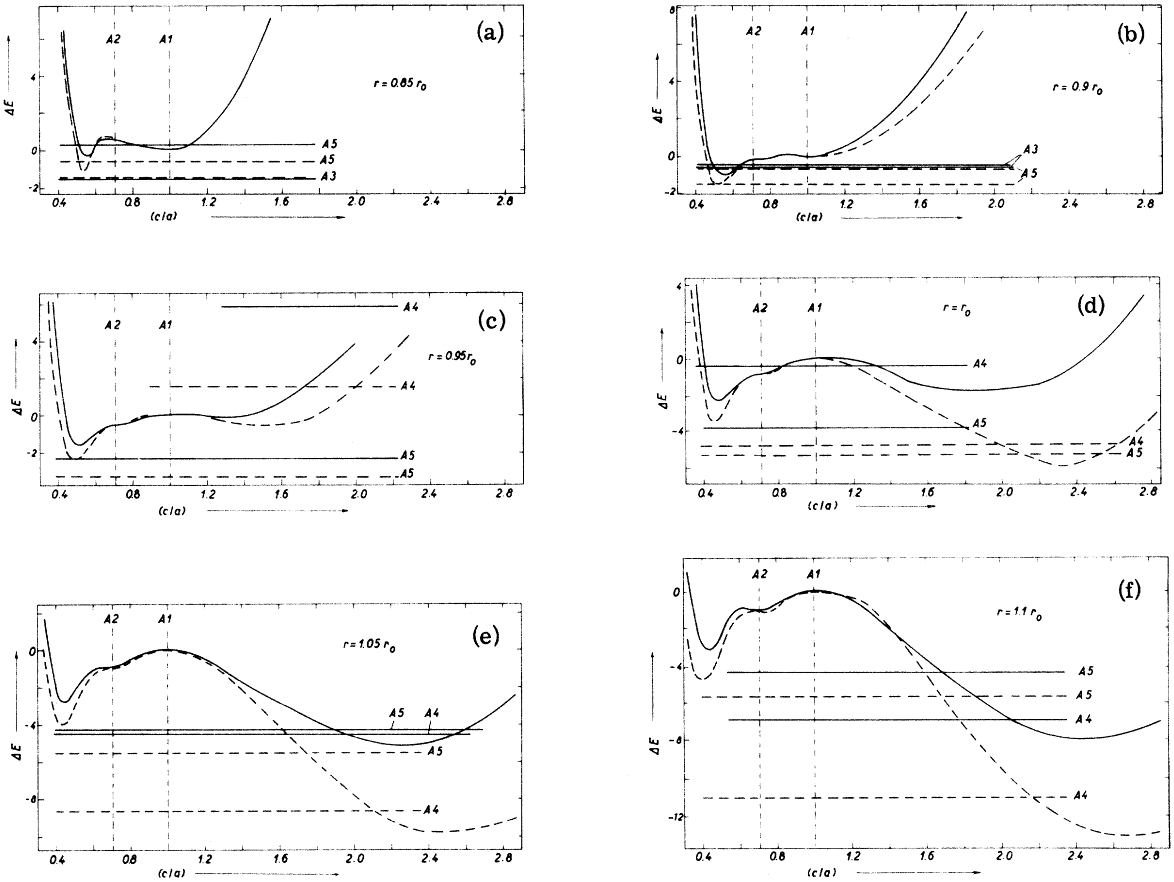

FIG. 6. Structural energy difference ΔE (in 10^{-2} Ry) relative to the $A1$ structure in an $A6$-type lattice as a function of the axial ratio c/a for different atomic radii r (r_0 is the observed atomic radius of white tin). Values of c/a corresponding to the $A1$ and $A2$ structures are indicated. The horizontal lines represent the relative energies of the $A3$, $A4$, and $A5$ structures. The solid curves refer to the results calculated with the Hubbard-Sham dielectric function, the broken curves to those calculated with the one of Singwi *et al.*

TABLE I. Energy differences relative to the $A1$ structure (in 10^{-3} Ry/ion) for different atomic radii r, calculated with different dielectric functions.

r/r_0		0.85	0.90	0.95	1.00	1.05	1.10	1.15
HS	$A2$	4.7	−1.6	−4.7	−7.3	−9.1	−7.1	
	$A3$	−14.5	−6.0	−5.7	−5.2	−4.6	−3.8	
	$A4$	280.5	151.3	61.9	−3.4	−44.3	−69.4	
	$A5$	2.6	−7.1	−26.1	−37.2	−42.4	−43.8	
	$A6^a$	−1.7	−8.8	−16.1	−21.1	−28.3	−31.8	−34.6
	(c/a)	(0.58)	(0.55)	(0.50)	(0.47)	(0.45)	(0.42)	(0.40)
SSTL	$A2$	5.0	−1.5	−5.0	−7.7	−9.9	−11.4	−11.6
	$A3$	−13.8	−6.5	−6.0	−5.7	−5.1	−4.3	−3.5
	$A4$	243.2	110.2	16.6	−46.7	−86.7	−109.6	−119.5
	$A5$	2.3	−13.1	−36.1	−50.5	−55.4	−56.1	−53.7
	$A6^a$	−5.7	−14.4	−23.5	−34.2	−40.8	−47.0	−52.7
	(c/a)	(0.54)	(0.50)	(0.48)	(0.44)	(0.42)	(0.40)	(0.38)

[a] The energy differences refer to the axial ratio minimizing the energy as given in the parentheses.

The interpolation techniques discussed in our previous papers[3] were used to join the computed points (seven points have been calculated for each structure) of the $E(\Omega)$ curve by a smooth line. At the absolute zero of temperature, the pressure of the system is given by the volume derivative of the energy, $p = -\partial E/\partial\Omega$, and the entropy contribution to H vanishes. The enthalpy difference at a given pressure p between two phases is represented by the distance between the intersection points of two parallel tangents to the $E(\Omega)$ curves with the energy axis [cf. Figs. 7(a) and 7(b)]. A pressure-induced phase transition occurs when the $E(\Omega)$ curves belonging to two different structures intersect. The transition will occur between the two phases at the points where the common tangent to the $E(\Omega)$ curves for the two phases touches the curves.[29] Our results, calculated with the Hubbard-Sham screening, are presented in Fig. 7(a), and those calculated with the Singwi-Sjölander-Tosi-Land dielectric function are shown in Fig. 7(b). The calculated equilibrium atomic radius of α-Sn is $r_0(\alpha) = 3.74(3.75)$ a.u., the binding energy is $E_B = -7.04(7.10)$ Ry. (Here and later in this chapter, the first theoretical value refers to the Hubbard-Sham screening function, and the second to that of Singwi *et al.*) This compares very favorably with the experimental values $r_0(\alpha) = 3.80$ a.u., $E_B = -7.00$ Ry, apart from the SSTL result for the binding energy. When the system is compressed, a phase transition occurs to the $A5$ structure, the atomic radius of the β phase being $r_0(\beta) = 3.58(3.48)$ a.u. (experimental $r_0(\beta) = 3.51$ a.u.). Taking the common-tangent construction and differentiating both $E(\Omega)$ curves, we calculate a critical pressure $p_c(A4 \rightarrow A5) = 15(220)$ kbar. Extrapolating the α-β phase boundary of Nikolaev *et al.*[12] from 77 to 0 °K, we deduce an experimental transition pressure of approximately 12 kbar. On further compression, a second phase transition occurs to the $A6$ structure, the axial ratio of the high-pressure phase Sn II being $c/a = 0.55(0.50)$ just after the phase change. For the atomic radius of the Sn II phase we calculate $r_0(\mathrm{II}) = 3.20(3.15)$ a.u. From the compression quoted by Barnett *et al.*[13] we estimate an experimental atomic radius of $r_0(\mathrm{II}) = 3.05$ a.u. Here again the agreement between theory and experiment is quite satisfying. However, if we proceed as above to calculate the critical pressure, we obtain $p_c(A5 \rightarrow A6) = 850(900)$ kbar against an experimental value of $p_c = 170$ kbar by extrapolating the β-Sn II-phase boundary data to the absolute zero of temperature. For the high-pressure $A3$ modification we obtain an atomic radius of $r_0(A3) \simeq 3.0$ a.u.; no attempt has been made to calculate the critical pressure for this transition. No experimental investigation of metallic tin at sufficiently high pressures is known up to now.

We are now to discuss the differences in our critical data calculated with the two different screening approaches and between theory and experiment. For this purpose, we consider the structural energy differences listed in Table I. It can be seen that the energy differences between the close-packed structures ($A1$, $A3$, and $A2$) are only very moderately affected by the choice of a dielectric function. On the other side, the energy differences between the $A4$, $A5$ lattices and the close-packed structures and between the $A4$ and $A5$ phases are much greater when the SSTL function is used [cf. also Figs. 3(a)–3(f)]. No direct comparison with experiment is possible, but we may deduce the structural enthalpy differences at zero pressure from our $E(\Omega)$ curves as indicated in Figs. 7(a) and 7(b). Our results are compiled in Table III together with the corresponding experimental data. We see that the HS approach yields a very good agreement for the enthalpy difference between the closely connected $A4$ and $A5$ structures, but overestimates the differences between these lattices and close-packed structures such as $A1$. In the SSTL approximation, the diamond lattice appears to be particularly favorable. This leads to a much higher critical pressure for the $A4 \rightarrow A5$ transition. The experimental enthalpy differences $\Delta H(A4 - A1)$, $\Delta H(A5 - A1)$ are rather uncertain and offer no measure for the Sn II-β-Sn enthalpy difference. The realistic lattice spacings for the Sn II phase obtained with our approach let us suppose the our energy differences are quite correct. On the other hand, the critical pressure is overestimated by a factor of 5. This is mainly due to a theoretical pressure-volume relation which is only semiquantitatively correct. The pressure-volume relation depends critically upon the variation of the structure-independent contribution E_{fe} to the binding energy (the so-called free-electron energy) with atomic volume, and this is the contribution which is the least accurately known. From our previous calculations[3] we know that the pressure is generally overestimated. In the case of tin an additional difficulty arises: For the correlation energy of the homogeneous part of the conduction-electron distribution, we use

TABLE II. Coordination number c and packing factor p for the different allotropic modifications of tin.

Structure	$A4$	$A5$	$A2$	$A3$, $A1$
c	4	6	8	12
p	0.34	0.535	0.680	0.740

the Nozières-Pines[30] formula. Now, for highly compressed tin, the density parameter r_s ($r_s = r_0/Z^{1/3}$) of the electron gas becomes smaller than 2 a.u. For $r_s \leq 2$ a.u. we are the borderline and even outside the applicability of the Nozières-Pines energy expression. The correlation energy and the total energy are underestimated and again the pressure is increased. Therefore the relatively inaccurate transition pressure for β-Sn-Sn II is not to be attributed to a deficiency in our structural energy calculation.

V. CONCLUSIONS

We have demonstrated that the phase changes in tin can be largely understood using the $X\alpha$-pseudopotential theory in terms of a delicate balance between the electrostatic energy preferring a body-centered-cubic arrangement of the ions, and the band-structure energy which favors the diamond lattice and produces a distortion of close-packed structures at lower and moderately high compression, whereas for extremely high

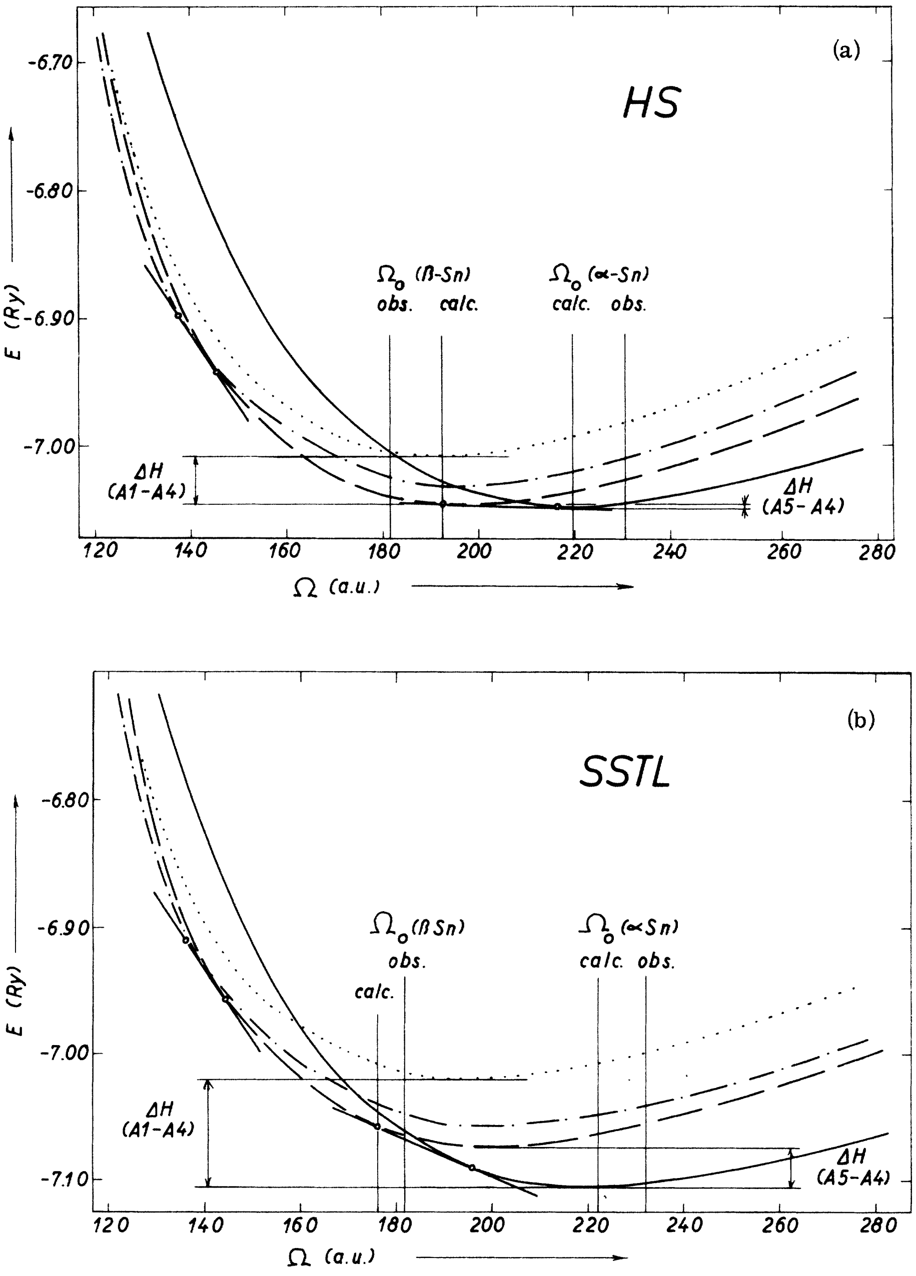

FIG. 7. Binding energy E as a function of the atom atomic volume Ω for different structures: solid curve, $A4$ (α-Sn); dashed curve, $A5$ (β-Sn); dot-dashed curve, $A6$ (SnII); dotted curve, $A1$. The common-tangent contruction for the pressure-induced phase transitions and the horizontal tangents yielding the zero-pressure enthalpy differences H are indicated. (a) Results calculated with the Hubbard-Sham (HS) screening function (b) with the one of Singwi *et al.* (SSTL).

TABLE III. Structural enthalpy differences $H(Ax-Ay) = H(Ax) - H(Ay)$ at zero temperature and pressure (in Ry/ion).

		$A4-A1$	$A5-A1$	$A4-A5$
Theory	HS	40.0	37.5	−2.5
	SSTL	85.0	53.4	−31.6
Experiment		5.9[a,b,c]	4.3[a]	−1.6[b,d]

[a] B. Predel and W. Schermann, A_c ta Metall. 19, 81 (1971).

[b] J. Lumsden, *Thermodynamics of Alloys*, Institute of Metals Monograph Series Vol. 11 (Institute of Metals, London, 1952).

[c] O. Alpaut and Th. Heumann, Acta Metall. 13, 543 (1965).

[d] J. N. Brönsted, Z. Phys. Chem. (Leipz.) 88, 479 (1914).

pressures it favors the structures with maximum packing density.

The phase transitions in tin provide a very sensitive test for any pseudopotential and for the applicability of a second-order perturbation approach. A second-order calculation is sufficient to reproduce the essential features of the structural transitions, though third-order terms might be necessary to remove the remaining very small instability of the diamond lattice against tetragonal distortion.

We have made a reasonable attempt to minimize the approximations underlying our theoretical approach, but uncertainties still persist. Uncertainties in the exchange and correlation interactions are largely responsible for the relative inaccuracy of our calculated critical pressures. Our use of the $\rho^{1/3}_{\text{core}}$ approximation to the conduction-band–core exchange potential has been justified by a number of successful calculations,[3,19,20] but still remains a somewhat uncertain approach. In this connection, lattice dynamical calculations are of interest. They should also contribute to our understanding of the microscopic phase stability. Such calculations are in preparation.

ACKNOWLEDGMENTS

The numerical calculations have been performed using the computing facilities of the Interfakultäres Rechenzentrum der Universität Wien (IBM 360/44) and the Rechenzentrum der Technischen Hochschule Wein (IBM 7040).

---

*Supported by the Fonds zur Förderung der wissenschaftlichen Forschung under Project Nos. 1318 and 2029.

[1] V. Heine and D. Weaire, *Solid State Physics*, edited by H. Ehrenreich *et al.* (Academic, New York, 1970), Vol. 24, p. 249.

[2] A. R. Williams and M. Appapillai, J. Phys. F 3, 772 (1973).

[3] J. Hafner, Phys. Status Solidi B 56, 579 (1973); 57, 101 (1973); 57, 497 (1973).

[4] T. Schneider and E. Stoll, Solid State Commun. 8, 1729 (1970); R. Pynn and I. Ebbsjö, J. Phys. F 1, 744 (1971).

[5] J. E. Inglesfield, J. Phys. C 1, 1337 (1968).

[6] Structure Reports, the continuation of the *Strukturbericht*, published for the International Union of Crystallography by N. V. A. OOsthoek's Uitgevers MIJ, Utrecht, The Netherlands.

[7] A. O. E. Animalu, Phys. Rev. 161, 445 (1967).

[8] J. Moriarty, Phys. Rev. B 8, 1339 (1973).

[9] W. A. Harrison, *Pseudopotentials in the Theory of Metals* (Benjamin, New York, 1966).

[10] J. Hafner, in Proceedings of the Fourth Annual Symposium on the Electronic Structure of Metals and Alloys, Gaussig, East Germany, 1974 (to be published).

[11] D. Weaire and J. E. Inglesfield, in *The Mechanism of Phase Transitions in Crystalline Solids*, Institute of Metals Monograph Series (Institute of Metals, London, 1969), Vol. 33.

[12] I. N. Nikolaev, V. P. Marlin, V. N. Panyushkin, and L. S. Pavlyukov, Fiz. Tverd. Tela 14, 2337 (1972) [Sov. Phys.-Solid State 14, 2022 (1973)].

[13] J. D. Barnett, R. B. Bennion, and H. T. Hall, Science 141, 1051 (1963).

[14] R. A. Stager, A. S. Balchan, and H. G. Drickamer, J. Chem. Phys. 37, 1154 (1962).

[15] M. J. P. Musgrave, J. Phys. Chem. Solids 24, 555 (1963).

[16] G. C. Kennedy and P. C. Newton, in *Solids under Pressure*, edited by W. Paul and D. M. Warschauer (McGraw-Hill, New York, 1963).

[17] K. A. Gschneider, *Solid State Physics*, edited by H. Ehrenreich *et al.* (Academic, New York, 1964), Vol. 16, p. 275.

[18] J. D. Dudley and H. T. Hall, Phys. Rev. 118, 1211 (1960).

[19] J. Hafner, Acta Phys. Austriaca 38, 70 (1973).

[20] J. Hafner and P. Schmuck, Phys. Rev. B 9, 4138 (1974).

[21] J. C. Slater and K. H. Johnson, Phys. Rev. B 5, 844 (1972), and references therein.

[22] K. Schwarz, Phys. Rev. B 5, 2466 (1972).

[23] I. Lindgren and K. Schwarz, Phys. Rev. A 5, 542 (1972).

[24] J. Hubbard, Proc. R. Soc. A 240, 539 (1957); 243, 356 (1957); L. J. Sham, *ibid.* 283, 33 (1965); N. W. Ashcroft, J. Phys. C 1, 232 (1968).

[25] K. S. Singwi, A. Sjölander, M. P. Tosi, and R. H. Land, Phys. Rev. B 1, 1044 (1970).

[26] E. G. Brovman and Yu. Kagan, Zh. Eksp. Teor. Fiz. 52, 557 (1967) [Sov. Phys.-JETP 25, 365 (1967)].

[27] C. A. Sholl, Proc. Phys. Soc. Lond. 92, 433 (1967).

[28] V. V. Evdokimova, Usp. Fiz. Nauk 88, 93 (1966) [Sov. Phys.-Usp. 9, 54 (1966)].

[29] J. W. Gibbs, *Collected Works* (Longmans and Green, New York, 1928).

[30] P. Nozières and D. Pines, Phys. Rev. 111, 442 (1958).